DOI: 10.1002/anie.201402560

Polymorphism

Thermally Driven Polymorphic Transition Prompting a Naked-Eye-Detectable Bending and Straightening Motion of Single Crystals**

Tatsuya Shima, Takahiro Muraoka, Norihisa Hoshino, Tomoyuki Akutagawa, Yuka Kobayashi, and Kazushi Kinbara**

Abstract: *The amplification of molecular motions so that they can be detected by the naked eye (10^7-fold amplification from the ångström to the millimeter scale) is a challenging issue in the development of mechanical molecular devices. In this context, the perfectly ordered molecular alignment of the crystalline phase has advantages, as demonstrated by the macroscale mechanical motions of single crystals upon the photochemical transformation of molecules. In the course of our studies on thermoresponsive amphiphiles containing tetra(ethylene glycol) (TEG) moieties, we serendipitously found that thermal conformational changes of TEG units trigger a single-crystal-to-single-crystal polymorphic phase transition. The single crystal of the amphiphile undergoes bending and straightening motion during both heating and cooling processes at the phase-transition temperatures. Thus, the thermally triggered conformational change of PEG units may have the advantage of inducing mechanical motion in bulk materials.*

Molecular single crystals are composed of perfectly aligned closely packed molecules. The regular, long-range aligned packing of molecules is advantageous for the development of optical and electronic devices with efficient charge transport, such as organic light-emitting diodes, transistors, and solar cells.[1] Such packing would also be favorable for the amplification of molecular motion to macroscale motion of bulk materials. However, it is known that the transformation of the molecular structure and/or conformation in a crystal usually produces local stress and often causes degradation and collapse of the single crystal.[2] Thus, stimuli responsiveness of the molecule should be compatible with elasticity of the crystal for the construction of mechanically functional crystalline materials.

In principle, heat can be expected to act as a stimulus to produce a mechanical motion of a single crystal by a thermal polymorphic transition. However, only limited examples of organic molecular crystals which show thermal single-crystal-to-single-crystal transitions with mechanical motion have been reported.[3] As a thermally responsive organic compound, poly(ethylene glycol) (PEG) is known to adopt different conformations, *gauche* and *anti*, at the C–C and C–O bonds at different temperatures.[4] In this context, we recently found that a cyclic PEG analogue consisting of tetra(ethylene glycol) (TEG) and pentaerythritol units exhibited a different physicochemical response from that of the noncyclic molecule.[5] Focusing further attention on the thermal responsiveness of PEG units, we synthesized an amphiphile, AT2B (Figure 1 a), composed of two TEG chains connecting *trans*-azobenzene and 1,4-bis(phenylethynyl)benzene (BPEB) units. Interestingly, AT2B exhibits a thermally induced reversible single-crystal-to-single-crystal polymorphic transition accompanied by a macroscopic bending and straightening motion, which is a different motion reported for photochemically driven transitions of single crystals.

AT2B was synthesized from 4,4′-(1,4-phenylenebis-(ethyne-2,1-diyl))diphenol, in which two hydroxy groups react with ditosylated TEGs, followed by azidonation of the unreacted tosyl termini.[6] A Huisgen cycloaddition with methyl 4-amino-2-ethynylbenzoate and oxidation of the resulting aniline units successfully afforded AT2B as an orange solid. Single crystals of AT2B were obtained as orange needles by a liquid–liquid diffusion method with *n*-hexane and tetrahydrofuran (THF) at 298 K.

Through differential scanning calorimetry (DSC) measurements, we observed a thermal transition of an AT2B crystal at a temperature lower than its melting point. A single crystal of AT2B was heated from 280 K at a rate of 1.0 K min^{-1} under N_2, and two endothermic peaks were observed at 333 and 422 K with enthalpy changes of $\Delta H =$ 2.4 and 50.3 kJ mol^{-1}, respectively (see Figure S1 in the Supporting Information). The melting point of the AT2B crystal was found to be 422 K by optical microscopic

[*] T. Shima, Dr. T. Muraoka, Dr. N. Hoshino, Prof. T. Akutagawa, Prof. K. Kinbara
Institute of Multidisciplinary Research for Advanced Materials
Tohoku University
2-1-1, Katahira, Aoba-ku, Sendai 980-8577 (Japan)
E-mail: kinbara@tagen.tohoku.ac.jp
Homepage: http://www.tagen.tohoku.ac.jp/labo/kinbara/index.html
Dr. T. Muraoka
Precursory Research for Embryonic Science and Technology
Japan Science and Technology Agency
4-1-8, Honcho, Kawaguchi, Saitama 332-0012 (Japan)
Dr. Y. Kobayashi
Advanced Key Technologies Division
National Institute for Materials Science
1-2-1 Sengen, Tsukuba, Ibaraki 305-0047 (Japan)

[**] We are grateful to Prof. Atsushi Muramatsu (Tohoku University) and Prof. Kiyoshi Kanie (Tohoku University) for their support with the DSC measurements and light microscopy. This research was partially supported by the Ministry of Education, Culture, Sports, Science and Technology of Japan (MEXT), Grants-in-Aid for Young Scientists S (21675003), Scientific Research on Innovative Areas "Spying Minority in Biological Phenomena" (No.3306; 23115003), and a Management Expenses Grant for National University Corporations to K.K.

Supporting information for this article is available on the WWW under http://dx.doi.org/10.1002/anie.201402560.

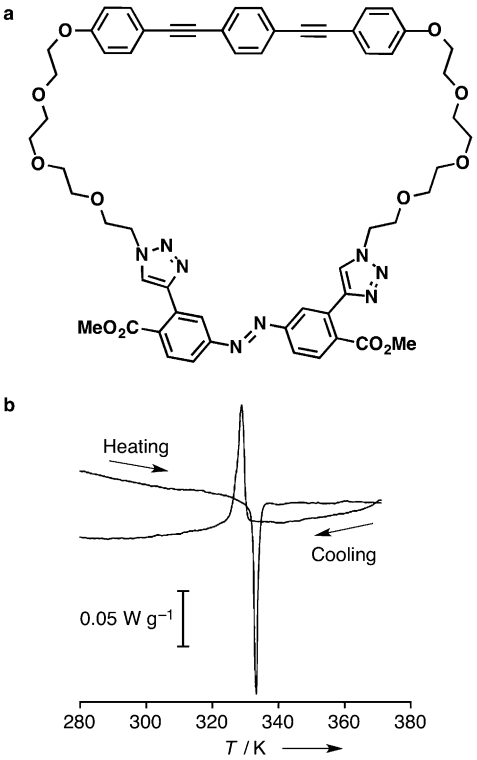

Figure 1. a) Molecular structure of AT2B. b) DSC profile of single crystals of AT2B during the first cycle of heating (280 to 370 K) followed by cooling (370 to 280 K) under a flow of N_2. Scan rate: 1.0 K min^{-1}.

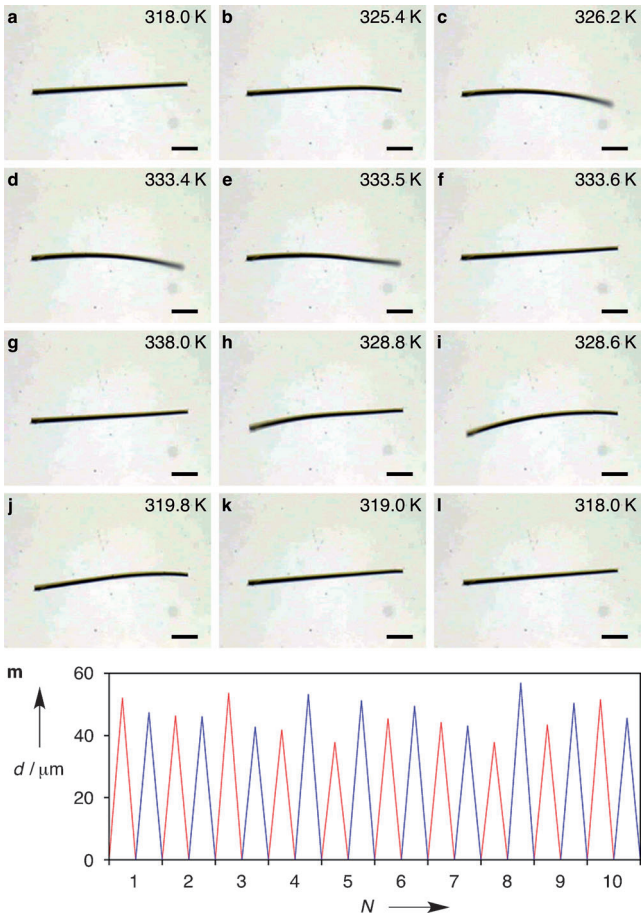

Figure 2. Snapshots of the single-crystal curving and straightening motions of AT2B upon a–g) heating and g–l) cooling between 318.0 and 338.0 K at a rate of 5.0 K min^{-1} on a hot stage under light microscopy. These micrographs were taken in the 10th cycle. The original movie is available in the Supporting Information (Movie S1). Scale bars: 100 μm. m) Displacement of a tip (*d*) of the single crystal in the projected image during the repeated heating (red lines) and cooling (blue lines) cycles (*N*) between 318.0 and 338.0 K.

observation. In the cooling process from the molten state (from 443 K), the DSC profile showed a single exothermic transition at 353 K with $\Delta H = 34.0$ kJ mol^{-1} (see Figure S1). Meanwhile, temperature reduction starting from 370 K (below the melting point) led to an exothermic peak at 329 K with $\Delta H = 3.1$ kJ mol^{-1}. The DSC profile was reversible over three cycles of heating and cooling (Figure 1 b).

Mechanical motion of the crystal during the heating and cooling processes was observed by optical microscopy. The crystallization of AT2B under liquid–liquid diffusion conditions with *n*-hexane and THF afforded a needle-shaped crystal (596 μm in length and 19.5 μm in width, obtained from a 2.0 mM solution in THF). Interestingly, when this crystal was heated on a hot glass stage at a rate of 5.0 K min^{-1}, the single crystal started to curve at 325.4 K, and reached a curvature of 23° with 53.7 μm tip displacement in the projection image (Figure 2 a–d; see Movie S1 in the Supporting Information). The bent single crystal returned to the straight morphology at 333.6 K (Figure 2 e–g; see Movie S1). During this bending motion, the tip moved out of focus, thus indicating that the tip turned up from the glass surface. In the cooling process from 338.0 K, the crystal again showed the bending and straightening motion (Figure 2 g–l; see Supporting Information, Movie S1). This motion could be repeated over 10 cycles with an average tip displacement of 47.1 μm (Figure 2 m). The crystal maintained homogeneous clarity under optical microscopic observation without any crack formation or decomposition before or after the macroscopic motions, thus suggesting that the crystal retains single crystallinity during the thermal process accompanied by a polymorphic transition.

By increasing the concentration of AT2B in THF to 10 mM, larger single crystals of 1.0 mm in width and 15 mm in length were successfully prepared. When the crystal was heated on a hot glass plate, a millimeter-scale bending and straightening motion was detectable even by the naked eye (Figure 3; see Movie S2). The crystal raised one edge by 1.6 mm from the glass surface owing to curving. Cooling of the crystal also triggered the millimeter-scale bending and straightening motion.

X-ray single-crystal analysis of AT2B was successfully performed at 273 (α phase) and 343 K (β phase) to enable visualization of the thermally induced polymorphic transition at the molecular level.[7] At 273 K, the space group of the crystal was *Pc* with the unit-cell parameters $a = 9.3125(2)$ Å, $b = 22.4838(4)$ Å, $c = 26.2684(6)$ Å, $\beta = 92.4750(10)°$, and $V = 5495$ Å^3. The asymmetric unit includes a pair of AT2B molecules (molecules A_α and B_α, Figure 4 a), which aligns

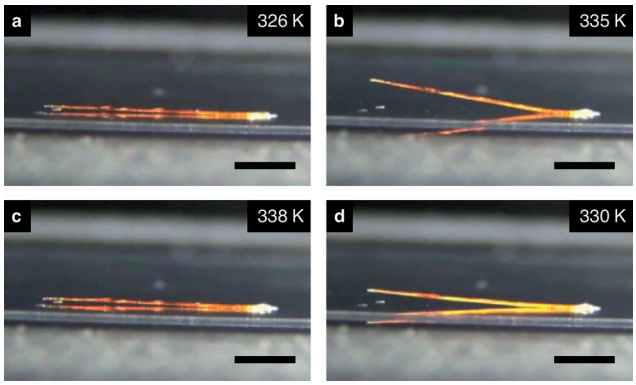

Figure 3. Snapshots of the macroscopic motion of a 15 mm long single crystal of AT2B on a hot stage during a–c) heating and c,d) cooling processes between 326.0 and 338.0 K. The original movie is available in the Supporting Information (Movie S2). One end of the crystal was adhered by glue. Scale bars: 5.0 mm.

alternately along the *c* axis with a glide plane and also stacks alternately along the *a* axis to form a columnar structure (Figure 4 a,b). The azobenzene and BPEB units align alternately along the *a* axis, where the intramolecular and intermolecular distances are 3.7 and 3.5 Å, respectively, thus indicating the presence of π–π interactions. It is notable that the needlelike single crystals grew in the direction parallel to the *a* axis. In the solid phase, the C–C and C–O bonds in a linear PEG are known to mostly adopts *gauche* and *anti* conformations, respectively.[4] The crystal structure of AT2B at 273 K showed that all C–C bonds in the TEG units of AT2B adopt the *gauche* conformation. However, unlike a linear PEG, 4 of the 14 C–O bonds in both molecules A_α and B_α adopt the *gauche* conformation, possibly because of the constrained cyclic molecular structure of AT2B.

The single crystal used for crystallographic analysis at 273 K was heated to 343 K, above the transition temperature, at a rate of 2.0 K min^{-1}, and crystallographic analysis of the second phase (β phase) was successfully performed. The space group was unchanged, and the lattice parameters (a = 9.5548(3) Å, b = 22.6356(7) Å, c = 25.9404(8) Å, β = 94.6350(9)°, and V = 5592.01 Å^3) revealed little change from those of the α-phase crystal.

Interestingly, C45 in molecule A_α, a carbon atom in the TEG chain near the triazole ring, flipped in this thermal transition to give conformation A_β (Figure 5 a; see Table S1 in the Supporting Information). C48 and C57 in the TEG chains close to the BPEB unit also flipped in this thermal transition. In contrast, the geometry and conformations of the azobenzene and BPEB units in molecule A hardly changed between the α and β phases, to allow retention of the π–π stacking. In a similar way, the TEG chains in molecule B exhibited conformational changes, whereas the aromatic units also retained a fairly unchanged geometry. As compared to the atoms in the azobenzene and BPEB units, the carbon and oxygen atoms in the TEG chains have larger atomic displacement parameters (ADPs) in the α-phase crystal (Figure 5 b; see Tables S2 and S3), thus suggesting that these atoms intrinsically have relatively high flexibility so that the thermally driven conformational change predominantly occurs around these portions of the molecule.

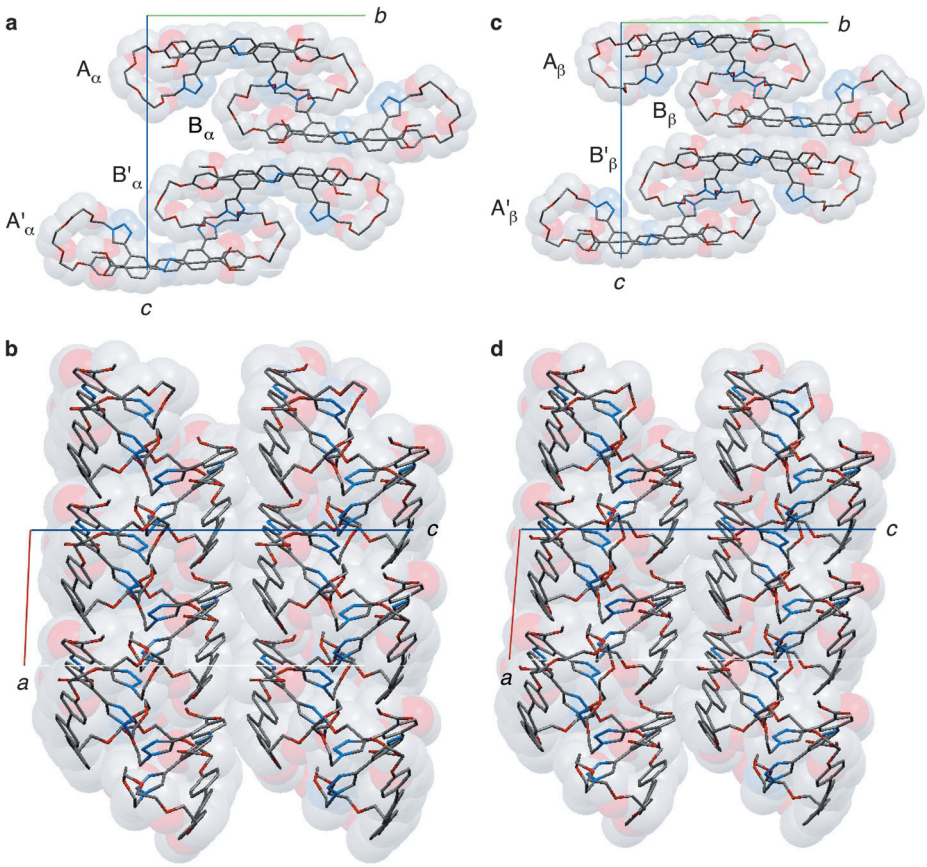

Figure 4. X-ray single-crystal structures of a,b) α- and c,d) β-phase crystals of AT2B viewed down the *a* axis (a,c) and the *b* axis (b,d). Carbon, nitrogen, and oxygen atoms are shown as gray, blue, and red, respectively. For clarity, hydrogen atoms are omitted.

Not only the conformations but also the alignment of the molecules changes in this polymorphic transition. In the transition from the α to the β phase, molecules A and B come close to each other along the *b* and *c* axes, which results in a change in the lattice parameters. The length of the *a* axis showed the largest expansion by 2.6%, whereas the *b* and *c* axes showed smaller expansion (0.68%) and contraction (1.2%), respectively. At the same time, the β value increased by 2.2° (2.3%). As discussed below, these differences in the lattice parameters are essential for generating the mechanical

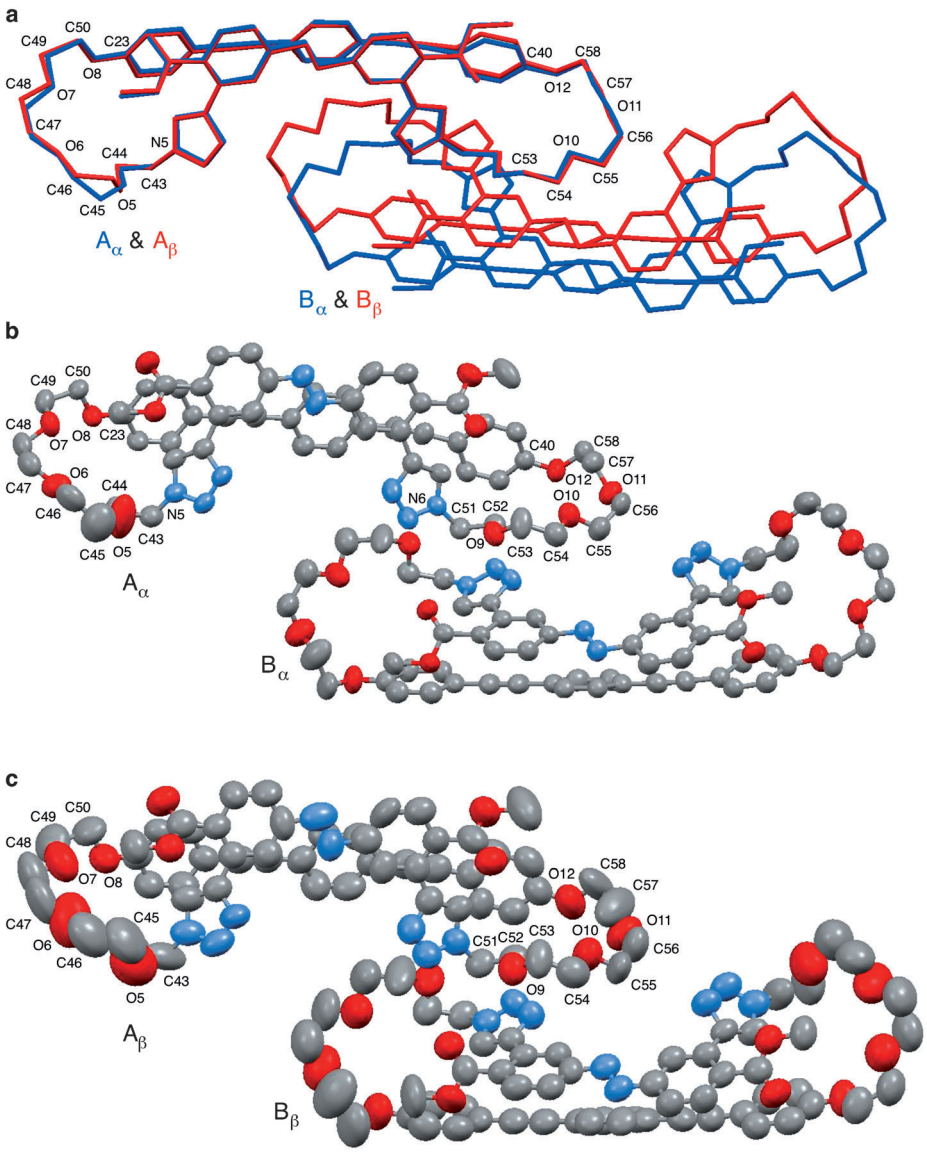

Figure 5. a) Merged X-ray crystal structures of AT2B in α- (blue, 273 K) and β-phase crystals (red, 343 K) viewed down the *a* axis. b,c) Thermal-ellipsoid plots shown at 50% probability of α- (b) and β-phase crystals (c). The atoms in the TEG chains of molecule A are labeled.

motions observed upon the heating and cooling of AT2B single crystals.

In the thermal polymorphic transition of AT2B, a hysteretic change in the dielectric constant of the single crystal was observed at the transition temperatures in the heating and cooling processes (Figure 6). The dielectric constant ε_r of a nonionic organic crystal depends on the degree of its spontaneous polarization toward an alternating electric field, and can also be correlated with the magnitude of the dipole moment.[8] A single crystal of AT2B in the α phase showed a dielectric constant $\varepsilon_r = 1.92$ at an alternating-electric-field frequency of 10^6 Hz at 273 K between (011) and $(0\bar{1}1)$ faces. The dielectric constant gradually increased with increasing temperature owing to the fluctuation gain of the molecule at higher temperatures (Figure 6). A discontinuous increment in the dielectric constant was observed at 335 K ($\varepsilon_r = 2.11$ and 2.37 at 333 and 339 K, respectively), corresponding to the phase-transition temperature observed by DSC (Figure 1). The dielectric constant further increased in response to the temperature elevation, with a similar slope to that below 333 K. In the cooling process, a discontinuous decrement in the dielectric constant was observed at 329 K ($\varepsilon_r =$ 2.37 and 2.11 at 332 and 327 K, respectively), which also corresponds to the phase-transition temperature. The change in the dielectric constant was hardly affected by the frequency of the alternating electric field between 10^4 and 10^6 Hz, thus suggesting that the thermal fluctuation of the dipole moments takes place at a frequency higher than 10^6 Hz. Theoretical calculations indicated that the dipole moment of each molecule in the asymmetric unit of the AT2B crystal (molecules A and B) changed upon the phase transition between the α and β phases: The calculated dipole moments are 2.5622 and 3.0261 D for molecules A_α and B_α, and 4.1245 and 2.6480 D for molecules A_β and B_β, respectively (see Figures S2 and S3 in the Supporting Information). On the other hand, the asymmetric unit has similar dipole moments for the α and β phases. These results suggest that although the thermally induced conformational change in the AT2B molecules possibly induces the change in the dipole moment at a molecular level, the observed change in the dielectric constants during the phase transition is probably due to the difference in the alignment of the molecules in the α and β phases.

Single crystals that undergo reversible macroscopic deformation triggered by light have been studied intensely by Irie and co-workers with dithienylethene derivatives, which undergo photochemical ring-opening and ring-closing reactions under UV and visible-light irradiation.[9] According to the mechanism proposed by Irie and co-workers for this phenomenon, a gradient in the distribution of open and closed forms, which cause shrinkage or expansion of the molecular packing, leads to the macroscopic bending motion of a single crystal. Since light cannot penetrate deeply into the crystal owing to the high absorbance and inner filter effect of the

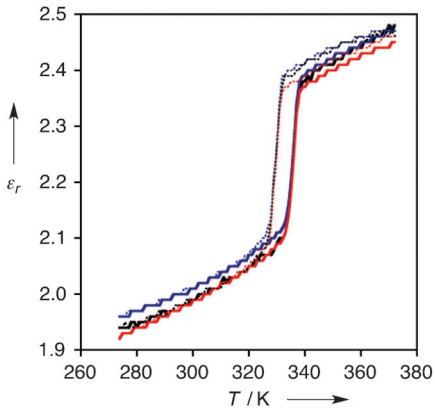

Figure 6. Dependence of the dielectric constant ε_r on the temperature upon heating (solid lines) and cooling (dot lines) between 273 and 372 K with alternating-electric-field frequencies of 10^4 (black), 10^5 (blue), and 10^6 Hz (red). Scan rate: 2.0 K min^{-1}.

densely packed molecules, photochemical reactions take place only at the thin surface layer exposed to light to produce a gradient distribution of open and closed forms between the inner and outer edges of the crystal and thus induce curving. For the straight morphology of the crystal to be restored, irradiation with light of a different wavelength that prompts the backward photochemical reaction is necessary.

In the case of the AT2B single crystal, it is considered that the thermally driven structural transformation of the molecules causes internal strain, which should start from the heated surface of the single crystal.[3d] Gradual release of the accumulated strain through the phase transition from the α to the β phase most likely leads to the deformation of the crystal. In this context, Naumov and co-workers reported that anisotropic distortion of the unit cell is a required factor to prompt a strong mechanical response.[3d] X-ray crystallographic analysis revealed that the length of the *a* axis extends by 2.6% through the phase transition from the α to the β phase, whereas the *b* and *c* axes show relatively small expansion and contraction, respectively. As mentioned above, the long axis of the needlelike single crystal is parallel to the *a* axis. Hence, it is likely that during the thermally induced phase transition between α and β phases, the anisotropic internal strain caused by the structural transformation is gradually released from the heated surface to the opposite side of the crystal, which translates into distortion of the crystal packing. Namely, the expansion of the *a* axis at the heated surface is likely to result in curving of the crystal along the *a* axis to raise a tip of the crystal from the hot stage. Unlike light,[9] heat can eventually be transferred to the whole crystal. Along with the propagation of heat, all or most of the molecules in the crystal could complete the transition so that the unit cells in the crystal again become homogeneous and the crystal is straightened; thus, a bending and straightening motion is observed. A similar phenomenon could also take place in the cooling process. This response is different from that of photoresponsive single crystals.

In contrast to the macroscopic single-crystal motions of photochromic molecules upon a bond-forming chemical reaction, the behavior of the system reported herein originates from the conformational change of the constituent molecules. The flexibility of the TEG chains attached to the π–π stacking rigid aromatic units enables partial mobility within the molecule and leads to the conformational change without collapse of the single crystallinity.[10] Thus, a PEG chain is considered to be a potential molecular unit for constructing thermally responsive crystalline materials. The conformational change of PEG would also cause a change in the dipole moment of a molecule, and possibly in the dielectric constant of the crystal, in response to thermal stimuli. This property would also be advantageous for the development of thermooptical devices.

Experimental Section

The single-crystal X-ray measurements for AT2B were conducted at 273 and 343 K by using a RAPID-II diffractometer (Rigaku) equipped with a Cu rotating anode fitted with a multilayer confocal optic ($\lambda = 1.54187$ Å). The RAPID-AUTO program (Rigaku) was used for cell refinement and data reduction. The crystal structures were solved by the direct method and refined with full-matrix least-squares methods on all F2 data by using the SHELX-2013 package (Sheldrick, 2013). Non-hydrogen atoms were refined with anisotropic thermal parameters. Hydrogen atoms were included in calculated positions and refined with isotropic thermal parameters riding on those of the parent atoms. The TEG parts in the crystal structures at 273 and 343 K were restrained because of the disorder.

The dielectric constant of a single crystal was measured by a Hewlett–Packard 4194A Impedance/Gain-Phase Analyzer through the two-probe alternating-current (AC) impedance method in the frequency range from 1.0×10^4 to 1.0×10^6 Hz. The electrical contacts were prepared by using gold paste (Tokuriki 8560) to attach gold wires with a diameter of 25 μm on (011) and $(0\bar{1}1)$ surfaces.

Received: February 18, 2014
Published online: May 30, 2014

Keywords: amphiphiles · conformational change · macrocycles · polymorphism · thermal responsiveness

[1] a) H. Alves, R. M. Pinto, E. S. Maçôas, *Nat. Commun.* **2013**, *4*, 1842; b) A. S. Tayi, A. K. Shveyd, A. C.-H. Sue, J. M. Szarko, B. S. Rolczynski, D. Cao, T. J. Kennedy, A. A. Sarjeant, C. L. Stern, W. F. Paxton, W. Wu, S. K. Dey, A. C. Fahrenbach, J. R. Guest, H. Mohseni, L. X. Chen, K. L. Wang, J. F. Stoddart, S. I. Stupp, *Nature* **2012**, *488*, 485–489; c) D. Braga, G. Horowitz, *Adv. Mater.* **2009**, *21*, 1473–1486; d) T. Takenobu, S. Z. Bisri, T. Takahashi, M. Yahiro, C. Adachi, Y. Iwasa, *Phys. Rev. Lett.* **2008**, *100*, 066601.

[2] M. A. Garcia-Garibay, *Angew. Chem.* **2007**, *119*, 9103–9105; *Angew. Chem. Int. Ed.* **2007**, *46*, 8945–8947.

[3] a) N. K. Nath, M. K. Panda, S. C. Sahoo, P. Naumov, *CrystEngComm* **2014**, *16*, 1850–1858; b) S. C. Sahoo, S. B. Sinha, M. S. R. N. Kiran, U. Ramamurty, A. F. Dericioglu, C. M. Reddy, P. Naumov, *J. Am. Chem. Soc.* **2013**, *135*, 13843–13850; c) M. Horie, Y. Suzaki, D. Hashizume, T. Abe, T. Wu, T. Sassa, T. Hosokai, K. Osakada, *J. Am. Chem. Soc.* **2012**, *134*, 17932–17944; d) S. C. Sahoo, M. K. Panda, N. K. Nath, P. Naumov, *J. Am. Chem. Soc.* **2013**, *135*, 12241–12251; e) Ž. Skoko, S. Zamir, P. Naumov, J. Bernstein, *J. Am. Chem. Soc.* **2010**, *132*, 14191–14202; f) M. Horie, T. Sassa, D. Hashizume, Y. Suzaki, K. Osakada, T. Wada, *Angew. Chem.* **2007**, *119*, 5071–5074; *Angew.*

Chem. Int. Ed. **2007**, *46*, 4983 – 4986; g) H. F. Lieberman, R. J. Davey, D. M. T. Newsham, *Chem. Mater.* **2000**, *12*, 490 – 494; h) P. Thuéry, M. Nierlich, R. Calemczuk, M. Saadioui, Z. Asfari, J. Vicens, *Acta Crystallogr. Sect. B* **1999**, *55*, 95 – 103; i) S. Zamir, J. Bernstein, D. J. Greenwood, *Mol. Cryst. Liq. Cryst.* **1994**, *242*, 193 – 200; j) J. Gigg, R. Gigg, S. Payne, R. Conant, *J. Chem. Soc. Perkin Trans. 1* **1987**, 2411 – 2414; k) M. C. Etter, A. R. Siedle, *J. Am. Chem. Soc.* **1983**, *105*, 641 – 643.

[4] a) M. Bjöerling, G. Karlstroem, P. Linse, *J. Phys. Chem.* **1991**, *95*, 6706 – 6709; b) H. Matsuura, K. Fukuhara, *J. Mol. Struct.* **1985**, *126*, 251 – 260; c) H. Matsuura, T. Miyazawa, *J. Polym. Sci. Polym. Phys. Ed.* **1969**, *7*, 1735 – 1744.

[5] T. Muraoka, K. Adachi, M. Ui, S. Kawasaki, N. Sadhukhan, H. Obara, H. Tochio, M. Shirakawa, K. Kinbara, *Angew. Chem.* **2013**, *125*, 2490 – 2494; *Angew. Chem. Int. Ed.* **2013**, *52*, 2430 – 2434.

[6] a) T. Muraoka, T. Shima, T. Hamada, M. Morita, M. Takagi, K. V. Tabata, H. Noji, K. Kinbara, *J. Am. Chem. Soc.* **2012**, *134*, 19788 – 19794; b) T. Muraoka, T. Shima, T. Hamada, M. Morita, M. Takagi, K. Kinbara, *Chem. Commun.* **2011**, *47*, 194 – 196.

[7] Crystal data for AT2B at 273 K: $C_{58}H_{58}N_8O_{12}$, MW = 1059.12, yellow prismatic, $0.20 \times 0.15 \times 0.15\ mm^3$, monoclinic, *Pc*, $a = 9.3125(2)$, $b = 22.4838(4)$, $c = 26.2684(6)$ Å, $\beta = 92.4750(10)°$, $V = 5495.0(2)$ Å^3, $Z = 4$, $\rho_{calcd} = 1.280\ g\,cm^{-3}$, $\mu = 7.49\ cm^{-1}$, $F_{000} = 2232$, $\theta = 3.368 – 68.136°$, < $Cu_{K\alpha}$, $\lambda = 1.54187$ Å, $T = 273(2)$ K, 18319 unique reflections ($R_{int} = 0.0746$), GOF = 0.981, $R1 = 0.0737$ ($I > 2\sigma(I)$), $wR2 = 0.1731$ ($I > 2\sigma(I)$). Crystal data for AT2B at 343 K: $C_{58}H_{58}N_8O_{12}$, $M_w = 1059.12$, yellow prismatic, $0.20 \times 0.15 \times 0.15\ mm^3$, monoclinic, *Pc*, $a = 9.5548(3)$, $b = 22.6356(7)$, $c = 25.9404(8)$ Å, $\beta = 94.6350(9)°$, $V = 5592.0(3)$ Å^3, $Z = 4$, $\rho_{calcd} = 1.258\ g\,cm^{-3}$, $\mu = 7.36\ cm^{-1}$, $F_{000} = 2232$, $\theta = 3.419 – 67.986°$, $Cu_{K\alpha}$, $\lambda = 1.54187$ Å, $T = 343(2)$ K, 18478 unique reflections ($R_{int} = 0.0630$), GOF = 0.961, $R1 = 0.1003$ ($I > 2\sigma(I)$), $wR2 = 0.2498$ ($I > 2\sigma(I)$). CCDC 969125 (273 K) and 969126 (343 K) contain the supplementary crystallographic data for this paper. These data can be obtained free of charge from The Cambridge Crystallographic Data Centre via www.ccdc.cam.ac.uk/data_request/cif.

[8] S. Horiuchi, Y. Tokura, *Nat. Mater.* **2008**, *7*, 357 – 366.

[9] a) M. Morimoto, M. Irie, *J. Am. Chem. Soc.* **2010**, *132*, 14172 – 14178; b) S. Kobatake, S. Takami, H. Muto, T. Ishikawa, M. Irie, *Nature* **2007**, *446*, 778 – 781.

[10] C. M. Reddy, M. T. Kirchner, R. G. Gundakaram, K. A. Padmanabhan, G. R. Desiraju, *Chem. Eur. J.* **2006**, *12*, 2222 – 2234.

